ISSN: 2454-9940

INTERNATIONAL JOURNAL OF APPLIED SCIENCE ENGINEERING AND MANAGEMENT

E-Mail :
editor.ijasem@gmail.com
editor@ijasem.org

www.ijasem.org

INTERNATIONAL JOURNAL OF APPLIED SCIENCE ENGINEERING AND MANAGEMENT

ISSN 2454-9940
www.ijasem.org
Vol 19, Issue 3, 2025

MODELLING AND IMPLEMENTING AN ISOLATED BIDIRECTIONAL DC-DC CONVERTER WITH THE PSO ALGORITHM FOR ELECTRIC VEHICLE POWER MANAGEMENT

Mr. G. YADAIAH
Department of Electrical & Electronics Engineering, Annamacharya Institute of Technology and Sciences, Hyderabad, Telangana, India
yadaiahacts08@gmail.com

Dr. U. Narender
Department of Electrical & Electronics Engineering, Annamacharya Institute of Technology and Sciences, Hyderabad, Telangana, India
narender@gmail.com

K. RAMESH
Research Scholar,
Department of Electrical & Electronics Engineering, Annamacharya Institute of Technology and Sciences, Hyderabad, Telangana, India
katravathramesh39@gmail.com

ABSTRACT- Once clean, renewable energy sources are used to charge the batteries in electric vehicles (EVs), the vehicles can produce zero gas emissions, greatly improving the environment. EVs and other distributed energy storage devices can be used in a smart micro grid to deliver energy to the loads throughout highest times, reducing the impact of load shading and improving the quality of the electricity. To achieve these goals of energy balance between EVs, the grid, and renewable energy sources, an isolated DAB DC-DC converter is required. This paper develops an optimized isolated DC-DC converter for controlling power flow in multiple directions in an EV. This converter contains a dc-dc bidirectional converter, dual active bridge converters. Additionally, the particle swarm optimization is developed to manage the power between the EV and the battery. In the planned technique, a bidirectional DC-DC converter can be considered to interconnect the EV battery towards deliver bidirectional power flow ability with the battery. The proposed approach is executed in MATLAB, and presentations are assessed by considering performance measures. Moreover, it is contrasted with the traditional approaches of particle swarm optimization (PSO).

Keywords: Triple active bridge, Modified coati optimization algorithm, bidirectional DC-DC converter, particle swarm optimization (PSO), solar energy

I. INTRODUCTION

Over the past two decades, EVs have garnered significant attention and increased in popularity globally as a highly talented other towards decrease greenhouse gas discharges in the transport sector [1]. Furthermore, new economic research indicates that electric vehicles (EVs) will soon completely replace internal combustion engine (ICEV) vehicles. This makes it necessary to build charging stations all over the world that can handle the demands for the substantial quantity of electricity required to charge these EVs. However, there becomes a problem with the infrastructure for charging EVs as the number of vehicles on the road develops [2]. Charging these vehicles using the current electric grid may become more challenging and may not be the best course of action. Consequently, there is an increasing need to create an EV charging infrastructure that is reliable [3], sustainable, and powered by renewable energy sources. Decreasing the burden on the traditional power grid and promoting a cleaner, more maintainable transport industry are just two advantages of switching to grid-based charging solutions [4,5]. Researchers studying power electronic interfaces for electric vehicle systems have published a wide range of papers in the literature [6]. We address various topologies of isolated multiport converters that are derived from multi-port converters. An isolated multi-port converter's conversion efficiency can be increased by applying the interleaving idea [7]. The output power of a multi-port energy converter is managed and regulated by the use of a single-leg active switching parameter. In the EV mentioned above, a dc/DC converter structure has been developed to analysis the energy transfer amid the battery and grid supply. This converter's switch count is dependent on the quantity of battery modules it contains [8]. For example, if there are 'n' battery designs, the architecture needs '2n' switches to function properly. An MCOA-based energy management technique has been suggested for efficient power management amid the grid source and battery as well as to overpower problems like overcharging of the grid source and excessive battery current during peak power [9]. This paper's primary contribution is outlined as follows: This paper develops an optimized isolated DC-DC converter for controlling power flow in multiple directions in an EV. This converter contains a DC-DC unidirectional converter, a bidirectional DC-DC converter, TAB, and a multi-port dual active bridge converter.

Additionally, the OC is developed to manage the power between the EV and the battery. The power flow is achieved by using the MCOA. In the MCOA, the optimal gain parameter of the converter is selected. In the planned technique, a bidirectional DC-DC converter can be considered to interconnect the EV battery towards deliver bidirectional power flow ability with the battery. The structure of the article's remaining part is as follows: The system's architecture and overview are described in section 2. The section on controller design is found in section 3. Section 4 and 5 presents the conclusions of the paper as well as the simulated outcomes.

A. existing works

Fuzzy Logic Control:

Overview: Fuzzy logic control utilizes human-like reasoning to manage system uncertainties and non-linearities. It is particularly beneficial in scenarios where precise mathematical modeling is challenging.

INTERNATIONAL JOURNAL OF APPLIED SCIENCE ENGINEERING AND MANAGEMENT
ISSN 2454-9940
www.ijasem.org
Vol 19, Issue 3, 2025

The design of a fuzzy logic controller requires a set of rules and membership functions, which can become complex and time-consuming to develop.

Computational Demand: The real-time application of fuzzy logic can impose significant computational demands, particularly in systems with high switching frequencies.

There are many linear controllers in the literature, such as H infinity controllers, proportional-resonant (PR) controllers, and proportional-integral (PI) controllers. There has also been discussion in the literature regarding the advancement of controllers based on soft computing. Stochastic dynamic programming-based power management for ZEZ drive readiness has been proposed by Jemin Woo et al. [10]. Its goal is to maximize HEV charging efficiency. Using future probability information up to an unlimited time horizon, stochastic dynamic programming uses a Markov chain to simulate the driver's intentions and creates optimal controllers. Effective charging is further made possible by the suggested controller's consideration of the distance to the zero-emission zone. Up to around 21% more fuel efficiency is achieved using the proposed power management method when compared to stochastic dynamic programming solutions that do not account for the remaining distance. Vinoth Kumar Manickam et al. [11] have presented a methodical methodology for managing power generators, electric car chargers, and battery chargers as a backup power source for electrical systems. This is made possible by accepting electric vehicles (EVs) as a useful element that possesses the ability to store, use, and generate energy. With the help of this feature, which enables the charger to operate in Grid-to-vehicle (G2V) and V2G modes at any power factor, the electric vehicle (EV) can perform a variety of grid support tasks in addition to charging, such as voltage control, RPC, and THD reduction.

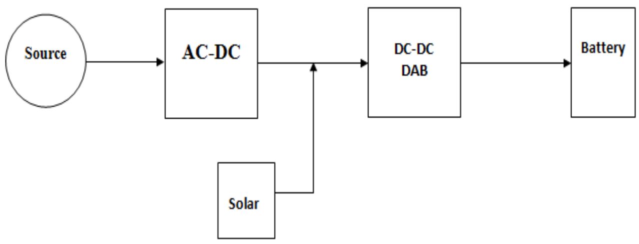

Fig. 1propsed block diagram

The Assailant Inspired Chimp Optimization Algorithm (AIChOa) is a novel method that maximizes the gain of the PI controller by applying the ideas of voltage synchronization, RPC, and THD reduction. Teja Barker et al. [12] have presented a carefully thought-out charging station design that works in unison with precision to optimize EV charging dynamics and neural network-based grid management. This is achieved by using Adaptive Neuro-Fuzzy Inference System (ANFIS) technology for voltage-controlled Maximum Power Point Tracking (MPPT) in conjunction with Type 3 and 2 controllers. To accommodate energy storage units (ESUs) and electric vehicles (EVs) across various power generations and demand scenarios, an adaptive sliding mode controller has been devised by R.S. Bajpai et al. [13]. By using a decentralized approach, the suggested adaptive sliding mode controller manages power distribution between the micro grid DC-link EVs and the ESUs. To confirm the sliding mode controller's effectiveness in battery charging applications, a thorough comparison between fuzzy logic and adaptive sliding mode control is conducted.

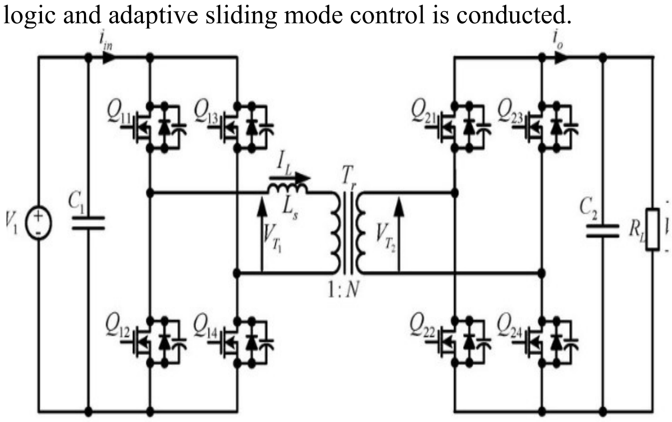

Fig.2. Architecture of the proposed model

The proposed model block diagram depicted in figure 1. The rest of the paper is organized as follows: Section II discusses the DAB with detailed mathematical analysis for the active power flow and RMS current calculations. Section III provides a detailed explanation and mathematical analysis for the PSO topology in addition to a closed-loop control algorithm to determine the optimum operating point for each DAB. Section IV provides steady state analysis in the results of DAB with PSO Concluded about project in Section V.

II. PROPOSED SYSTEM

A. Proposed DC-DC converter

Energy scarcity and environmental deterioration have garnered more attention in the past few years. The pollution caused by car exhaust emissions has increased with more people owning cars, which have forced an acceleration of the energy transition in automotive energy. Conventional EV energy storage systems are battery-powered storage devices with several drawbacks and shortcomings. At first, while an EV is rising or accelerating, its battery's power density is insufficient to fulfil its peak power requirement. Furthermore, the EV load will significantly increase as the power requirement is offset by adding more battery cells. To control power flow, this study proposes an optimized isolated DC-DC converter and an ideal charging and discharging controller for EVs to create a rapid charging system. In figure 2, a dual active bridge, a DC-DC bidirectional converter, and a bidirectional DC-DC converter are all combined in this section to provide the converter's full functioning mode.

Using fundamental harmonic analysis, DAB equivalent circuit is depicted in Figure 3, where each side of the DAB is replaced by a fundamental AC source. The RMS phasor of the fundamental voltage component at both sides (1 and 2) V_ 1 and V_2 can be represented

The fast-charging system, which enhances the charging and discharging processes, provides the battery with maintenance. Furthermore, the battery is coupled with the grid to supply the necessary energy if the battery can be unable to sustain the load of electric vehicle. This is achieved by designing the controller assisted optimized isolated DC-DC converter. Power management control's primary function is to balance out load demand by taking into account the battery's charging and discharging controller, which is determined by MCOA. The suggested strategy to extend battery life is energy management and charging using a discharge controller, which lowers the risk of overcharging and drying up the battery. There are two ways to use the grid to improve the battery. The grid is used in condition 1 to charge the battery when it is

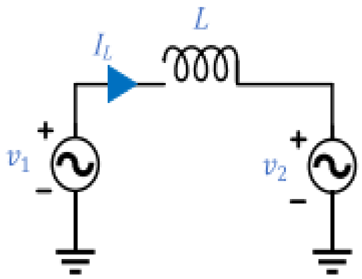

Fig. 3 DAB fundamental harmonic analysis equivalent circuit.

empty and to store extra energy when the battery is overcharged. The system model and system modelling are shown in the parts below.

III. THEORY AND CALCULATION

A. Modelling of Electrical Vehicle

When driving at different speeds, an EV needs a certain amount of energy to accelerate and brake. The amount of energy consumed by the EV depends on the energy requirements of the vehicle. In addition, the rolling friction force and aerodynamic resistance can exert their respective forces on a moving vehicle. Forces in an EV are related to several different things, including tire pressure [14], vehicle shape, pavement type, tire width and frontal surface. The vehicle is experiencing a resultant force that causes a velocity change that is connected to the instantaneous velocity under consideration and is reasonably easy to compute. Following that, driving force is typically used to calculate a vehicle's energy demand (DF). Furthermore, the difference in rolling resistance (RR), resultant force (RF), and aerodynamic resistance (AR) is what is referred to as the EVs.

$$DF = RF - AR - RR \quad (1)$$

The following formula is used to get the EV's RR:

$$RR = (1 + kv\ 2) \quad (2)$$

Here, $Fto$is a low-speed resistance coefficient, G is the standard gravity acceleration, V is the vehicle speed, M is a vehicle mass, is the rolling resistance coefficient. After the drag racing test is validated, the low-speed coefficient is computed and expressed as follows:

$$Fto = vb2\ 2gst \quad (3)$$

Here, vb is the initial speed of the vehicle and st Is a rolling distance of the vehicle. The low speed with RR coefficient for an EV travelling normally on the road is seen as falling between 0012 and 0014.

$$AR = 1/2\ \rho cxavr\ 2 \quad (4)$$

$$e = DFs/\eta \quad (5)$$

$$p = DFv/\eta \ or\ P = e/T \quad (6)$$

Here, ρ is an air density, cx is a longitudinal direction through an air resistance coefficient correlated to vehicle shapes then ranges, A is defined as a vehicle coefficient of frontal superficial location, 2 is the vehicle speed correlated to the air. The thermal resistance parameter, the car's instantaneous velocity, and the assumed drive architecture efficiency within the specified stage are used to calculate the EV's driving force together with the energy and instantaneous power needed to specify route S in a specific amount of time.

B. Modelling of Battery

Because of their life cycle, batteries connected to lithium-ion technology are frequently used in EVs. For lithium-ion battery simulation, the internal resistance model is taken into consideration because of its simple and accurate information representation. The battery's internal resistance model comprises an ideal cell with an internal resistance and an internal resistance with a series cell [15].

$$P_B = V_{OC} I_B - R_{IN} I_B^2 \quad (7)$$

$$I_B = \frac{V_{OC} - \sqrt{{V_{OC}}^2 - 4P_B R_{IN}}}{2R_{IN}} \quad (8)$$

$$V_B = V_{OC} - R_{IN} I_B \quad (9)$$

$$V_B = \frac{V_{OC} - \sqrt{{V_{OC}}^2 - 4P_B R_{IN}}}{2} \quad (10)$$

Whether the battery is charging or draining affects its internal resistance. The formula for the battery current, terminal voltage and output power is as follows:

Here, VOC is an open circuit voltage, RIN is an internal resistance, is a terminal current, VB is a terminal voltage and PB is a battery output power. Calculating the quantity of charge that remains in the battery for use allows one to estimate the amount of energy that is saved. The state of charge (SOC) of a battery is its volume of accessible charge at its maximum charge capacity. Charging loss is quantified using the coulombic efficiency. The battery's SOC during charging and draining is represented by the following dynamic equation:

$$SOC = \begin{cases} -\frac{I_B}{C_{ah}} & I_B \geq 0 \\ -\frac{C_{eff} I_B}{C_{ah}} & I_B < 0 \end{cases} \quad (11)$$

Here, Cef is the Coulombic efficiency, I_B is a battery temperature and Cah is the maximum capacity of a battery.

C Switching Operation:

As shown in Fig. 3, the switching cycle of the converter can be divided into 6 operation modes as follow:

(1) Mode 1 (t0 − t1)

As shown in Fig. 3a, the inductor current iL is in the negative direction. At t0, the S1 and S2 are turned ON in the primary bridge, and S5 and S7 are turned ON in the secondary one. According to the current direction, the current fows through S2 and D1 in the primary bridge and through S5 and D7 in the secondary one. Vh1 and Vh2 are zero at this moment; thus, the voltage through L becomes zero and a constant current fows through the inductor at iL = iL0.

(2) Mode 2 (t1 − t2)

Figure 3b displays the equivalent circuit of mode 2. Te current is still in the negative direction. S1, S4, S5, and S7 are

ISSN 2454-9940
www.ijasem.org
Vol 19, Issue 3, 2025

turned ON. According to the current direction, the current fows through D1 and D4 in the primary bridge and through S5 and D7 in the secondary one. Vh1 is clamped to V1 while Vh2 is still zero; therefore, the voltage through L is clamped to V1. In this mode, the current decreases linearly and can be expressed as:

(3) Mode 3 (t2 − t3)

Figure 3c shows the equivalent circuit of mode 3. Te current polarity changes from negative to positive. In this mode, S1 and S4 are still turned ON and S5 and S6 are turned ON. According to the current direction, the current fows through S1 and S4 in the primary bridge and through D5 and D6 in the secondary one. Vh1 is still at V1 while Vh2 is clamped to nV2. Hence, the voltage through L is clamped to V1 − nV2.

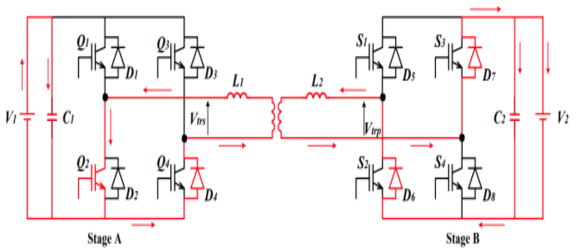

(a) Mode1:

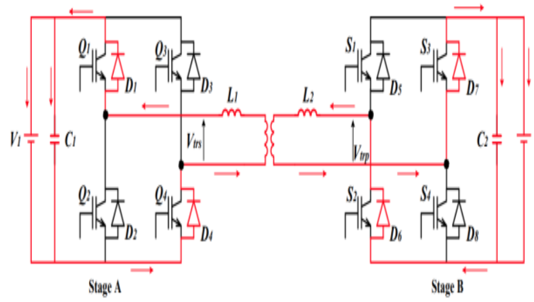

(b) Mode2:

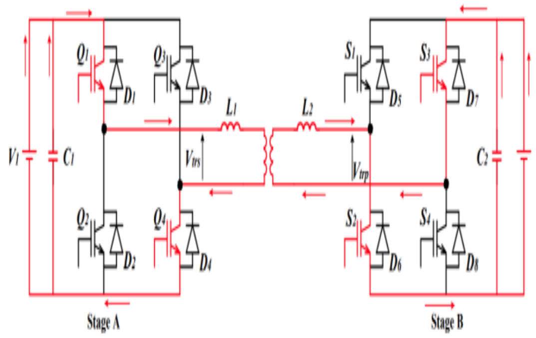

(c) Mode 3:

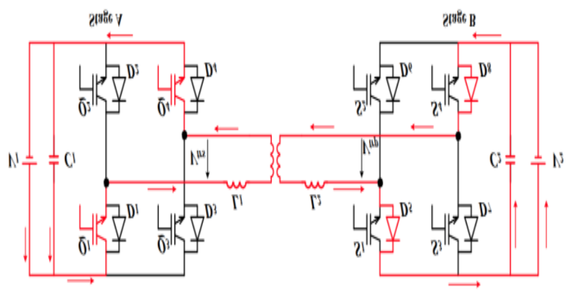

(d) Mode 4:

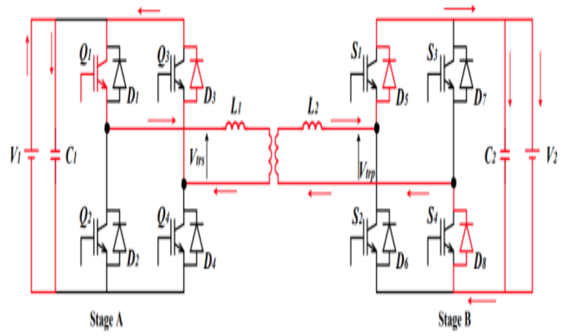

(e) Mode 5:

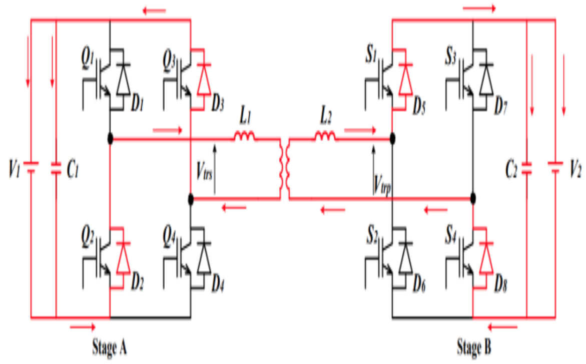

(f) Mode 6:

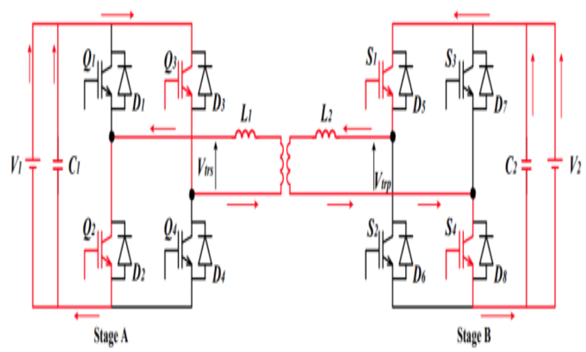

(g) Mode 7:

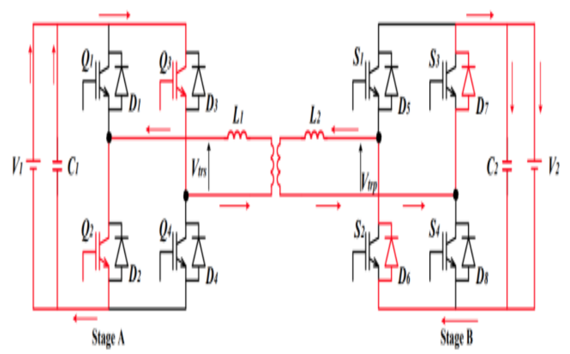

(h) Mode 8:

Fig. 4 Individual Mode of operations of the Bidirectional Converter

(4) Mode 4 (t3 − t4)

Figure 4d illustrates the equivalent circuit of mode 4. As shown from the waveforms in Fig. 5, mode 4 is similar to mode 1; iL is in the positive direction. At t3, S3 and S4 are turned ON while S8 and S6 are turned ON. According to the

ISSN 2454-9940
www.ijasem.org
Vol 19, Issue 3, 2025

current direction, the current fows through S4 and D3 in the primary bridge and through S8 and D6 in the secondary one. Since Vh1 and Vh2 are zero, the voltage through L becomes zero and the current is fxed at iL = iL3.

(5) Mode 5 (t4 − t5)

Figure 3e displays the equivalent circuit of mode 5. Te current is still in the positive direction. S2 and S3 are turned ON while the switches S6 and S8 are turned ON. According to the current direction, the current fows through D2 and D3 in the primary bridge and through S8 and D6 in the secondary one. Vh1 is clamped to − V1 while Vh2 is still zero; thus, the voltage through L is clamped to − V1.

(6) Mode 6 (t5 − t6)

Figure 3f shows the equivalent circuit of mode 6. Te current polarity changes from positive to negative. S2 and S3 are still turned ON and the switches S7 and S8 are turned ON. According to the current direction, the current fows through S2 and S3 in the primary bridge and through D7 and D8 in the secondary one. Vh1 is still at − V1 while Vh2 is clamped to − nV2. Therefore, the voltage through L is clamped to −V1 + nV2.

These switching conditions are investigated for each time intervals and iL1 is calculated for them as shown below;

Mode 1 (t0 t1):

$$i_{L1}(t) = i_{L1}(t_0) + \frac{nV_2}{L_1}(t - t_0)$$

Mode 2 (t1 – t1'):

$$i_{L1}(t) = i_{L1}(t_1) + \frac{V_1 + nV_2}{L_1}(t - t_1)$$

Mode 3 (t1' – t2):

$$i_{L1}(t) = i_{L1}(t_1) + \frac{V_1 + nV_2}{L_1}(t - t_1{}')$$

Mode 4 (t2 – t3):

$$i_{L1}(t) = i_{L1}(t_2) + \frac{V_1 - nV_2}{L_1}(t - t_2)$$

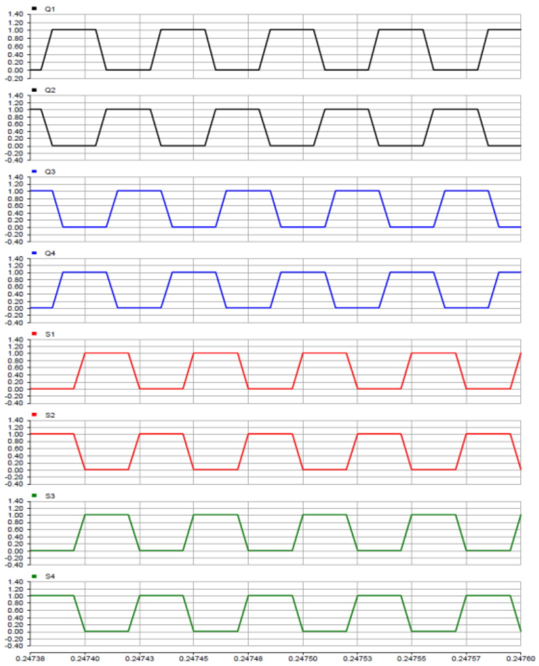

Fig 5.Switching conditions of the each time intervals in different modes.

Mode 5 (t3 – t4):

$$i_{L1}(t) = i_{L1}(t_3) + \frac{-nV_2}{L_1}(t - t_3)$$

Mode 6 (t4 – t4'):

$$i_{L1}(t) = i_{L1}(t_4) + \frac{-V_1 - nV_2}{L_1}(t - t_4)$$

Mode 7 (t4' – t5):

$$i_{L1}(t) = i_{L1}(t_3) + \frac{-nV_2}{L_1}(t - t_3)$$

Mode 8 (t4' – t5):

$$i_{L1}(t) = i_{L1}(t_5) + \frac{-V_1 + nV_2}{L_1}(t - t_5)$$

C. PARTICLE SWARM OPTIMIZATION (PSO)

A steam turbine is a machine that converts thermal energy of pressurized steam to mechanical energy in the form of rotary motion. From traditional fossil fuel based power plant to nuclear power plant steam turbine is a widely used prime mover. It normally operates at 3600 rpm speed while in the nuclear industry it runs at 1800 rpm speed. The control of the turbine is indispensable, as turbines need to be run up slowly, to prevent damage as well as require precise speed control to follow the generator load variation. The control system and protection are separate although they have the same system with Controller/Governor, actuator with arm and series valves. The speed throughout the operation of the system needs to be controlled by the governor. The governor gets input signals from the generator, the turbine shaft, the steam main output (input for turbine) pressure and the steam outlet/extraction pressure of the turbine.

The crossover and mutation; the two main operations of GA cannot guarantee better fitness of offspring as the chromosomes in the population have similar structure and their average fitness are high toward the end of the evolutionary process. Kennedy and Eberhart developed one of the modern heuristic algorithms known as PSO that has been stirred by the behavior of organisms, such as fish schooling

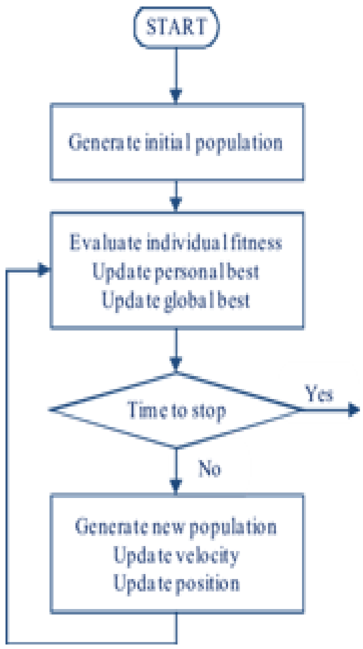

INTERNATIONAL JOURNAL OF APPLIED SCIENCE ENGINEERING AND MANAGEMENT
ISSN 2454-9940
www.ijasem.org
Vol 19, Issue 3, 2025

Fig. 6 Flowchart for particle swarm optimization algorithm.

and bird flocking. Members of fish schooling or bird flocking follows an inherent rules to undertake a synchronized movement so that they don't collide.

A particle swarm optimization (PSO) flowchart visually represents the algorithm's steps. It starts with initializing a swarm of particles, then iteratively updates their positions and velocities based on their own best experience and the best experience of the swarm. This process continues until a termination condition is met, such as reaching a maximum number of iterations or achieving a satisfactory fitness value.

This phenomenon is used to optimize the complex solutions using PSO. PSO is characterized as easy to execute, and computationally proficient heuristic technique. This algorithm in comparison to GA has a faster speed and faster premature convergence. It also has a flexible and well-balanced mechanism to improve the exploration abilities. In PSO, the particles are updated according to their current positions and velocities. The prospective solutions, called particles, fly through the problem space following the current optimum particles.

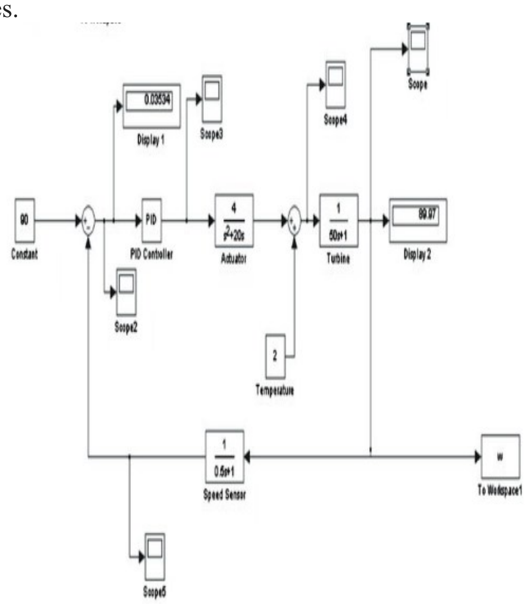

Fig. 7 PSO based PI Controller Design

The position of a particle represents a candidate solution to the optimization problem. Each particle within the space changes its velocity and position according to rules originally motivated by behavioral models of bird flocking. Each time it identifies a better fitness value, stores it and represents it as pbest. It continues an iterative process and finally updated two best values; one is pbest and the other one gbest, the global best throughout the population.

The proportional-integral-derivative (PID) controller is utilized in this design and latter tuned using PSO and GA.

$$u(t) = K_p e(t) + K_I \int_0^t e(t)\,dt + K_D \frac{de(t)}{dt} \quad (1)$$

In this control algorithm, P corresponds the proportional term

$$K_p e(t),$$

Where

K_p is the proportional gain of the controller. Similarly, I represent the integral term

$$K_i \int_0^t e(t)\,dt$$

And D stands for the derivative term $K_d \frac{de(t)}{dt}$ of the controller. K_i and K_d are integral and derivative gain of the controller, respectively.

The transfer function of the PID controller is as follows,

$$K_p + \frac{K_i}{s} + K_d s = \frac{K_p s + K_i + K_d s^2}{s} \quad (2)$$

Using these three terms, the controller by adjusting the process control input $u(t)$, minimizes the error value. The weighted sum of the three components is used to adjust the process by a control element, as in the steam turbine control a flow control valve.

Design Optimization Tools

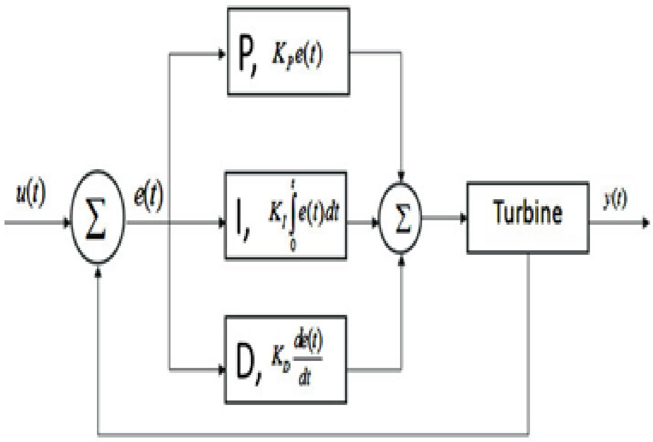

Fig. 8 Block diagram of a PID control

In this paper, the PID controller is optimized to achieve the optimal behaviour of the plant. The optimizer is used to search for the optimal solution of the PID control gains K_p, K_i, and K_d. Intelligent optimization algorithms are appropriate choices in selecting an optimizer. The proposed methodology utilizes Particle Swarm Optimization (PSO) tools. To investigate the effectiveness of utilization of PSO in respect to Genetic Algorithm (GA), the numerous simulations of both the techniques have been performed and the results are compared.

IV. RESULTS AND DISCUSSIONS

The performance of the suggested approach is examined and verified in this section. The suggested approach was created to strengthen the EV battery's quick charging mechanism. By considering the suggested rapid charging controller, this suggested methodology extends battery life. The rapid charging controller is used to manage the battery to extend its life. This controller allows for appropriate EV load demand adaptation during charging and discharging. Performance analysis and comparison are used to assess the suggested method's

ISSN 2454-9940
www.ijasem.org
Vol 19, Issue 3, 2025

implementation in MATLAB. The design parameter assumption is used to validate the proposed method's comparison. The battery and the suggested controller performance computation are validated by taking into account the EV load.

Table-I
Simulation parameters

Input voltage	440
Inductance	10mh
Capacitance	100micro F
Battery SoC	20%
Switching frequency	1000F
Solar voltage	100v

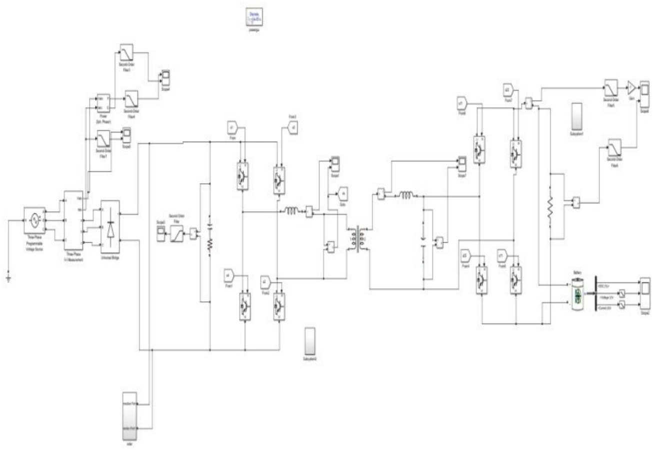

(a)

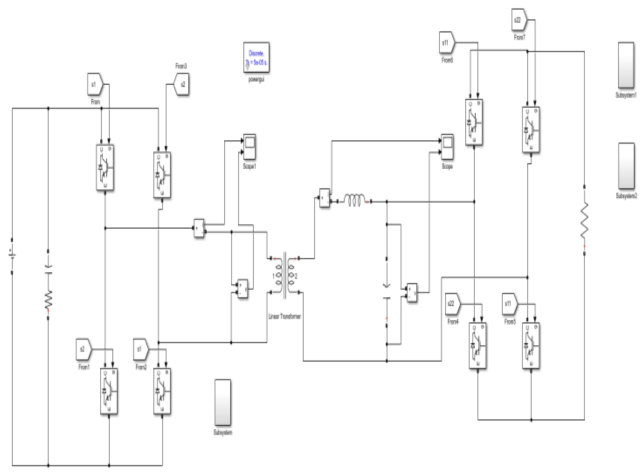

(b)

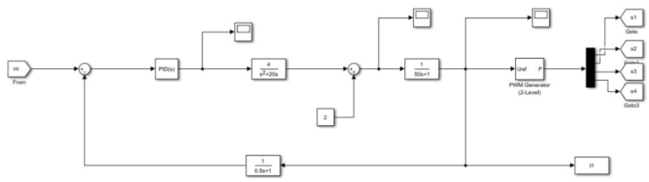

(c)
Fig. 9 (a) Simulink full diagram (b) DC-DC diagram (c) control diagram

Figure 9 displays the suggested methodology's Simulink diagram. The EV is first built with speed-related load conditions. Energy is used, and the battery is charged and discharged following the vehicle load.

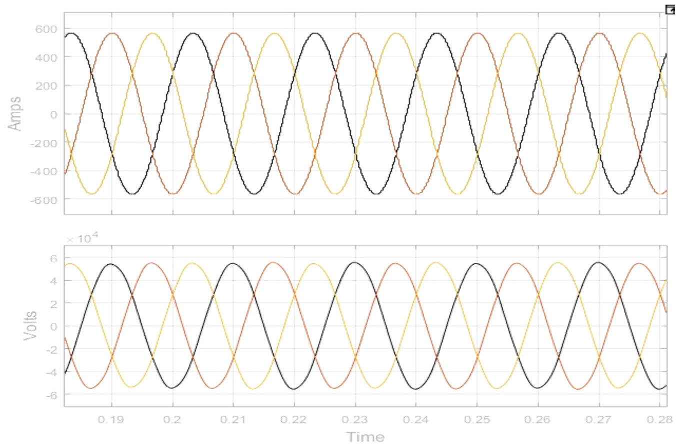

Fig. 10 grid input voltage

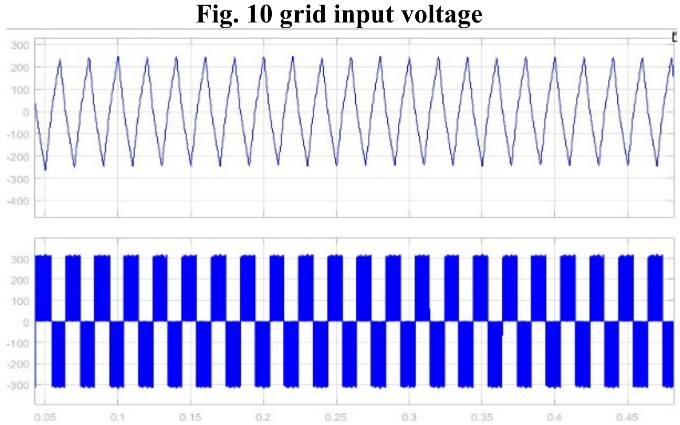

(a)

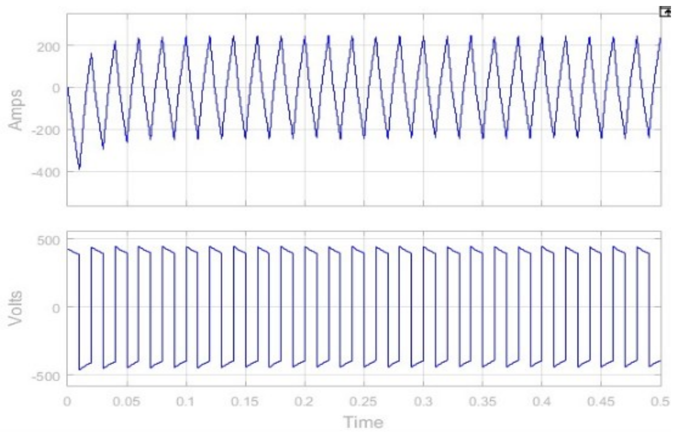

(b)
Fig. 11 (a) primary voltage and current, (b) secondary voltage

INTERNATIONAL JOURNAL OF APPLIED SCIENCE ENGINEERING AND MANAGEMENT
ISSN 2454-9940
www.ijasem.org
Vol 19, Issue 3, 2025

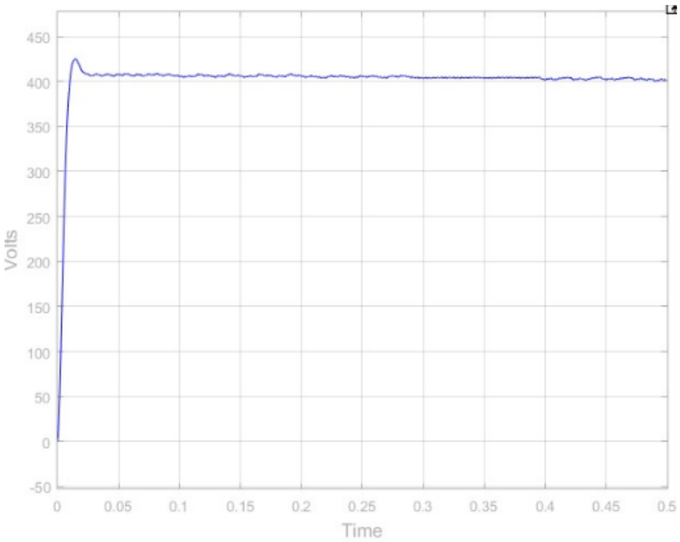

Fig. 12 Dc voltage

Figure 10 declares the HB1 supplied ac values, and the input voltage is 400dc. In a similar vein, the EV uses less energy and has a slower pace because it is powered by hb2 to the battery. This procedure is used to balance the load using battery energy storage devices. The battery keeps charging and discharging in order to make up for the required load. This procedure results in the EV's battery issues and reduced battery life. A quick charging controller was created to improve the performance of batteries. There are various types

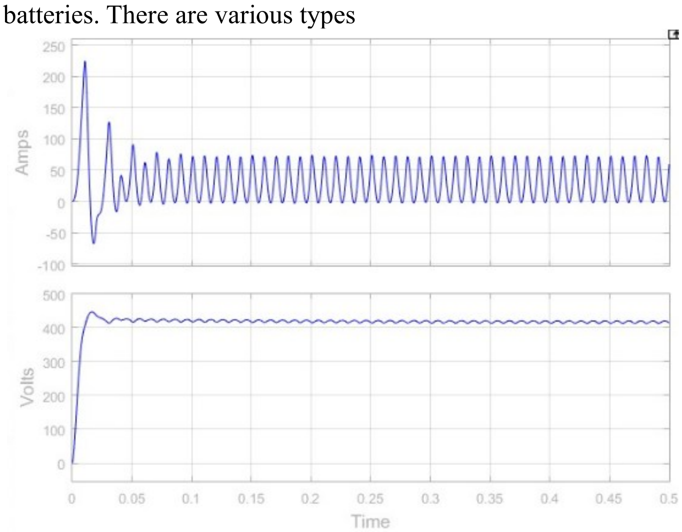

Fig.13 output voltage

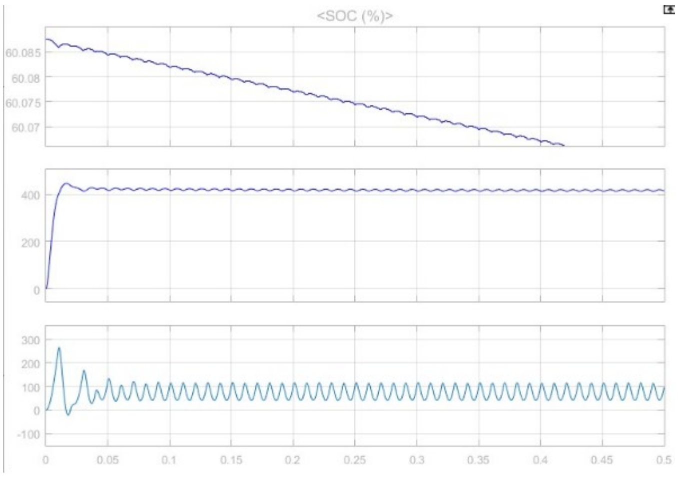

Fig. 14 battery voltage and soc

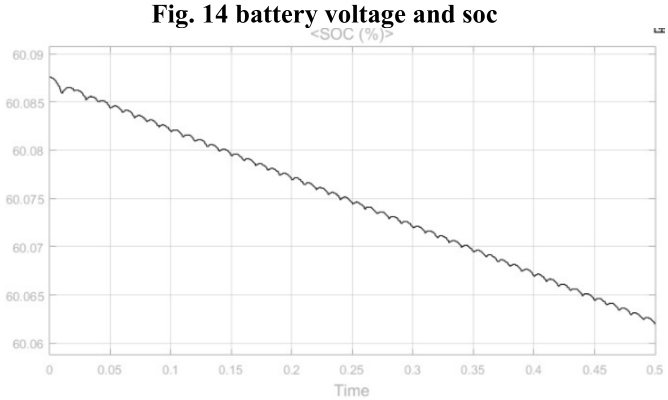

Fig. 15 Battery soc in solar mode

of losses associated with an electric vehicle load, including electrical losses from batteries, generators, motors, and total losses. Based on simulation

TABLE -2
Comparison between FUZZY and PSO controller

	FUZZY	PI with PSO
Input voltage	400	400
Dc link voltage	290	310
Battery SOC	60 – 59.9	60.09-60.06
Battery voltage	400	400
Battery Current	40	40
Primary voltage	400	300
Secondary voltage	400	400

results, demonstrates that Particle Swarm Optimisation(PSO) consistently outperforms fuzzy controllers in terms of solution quality, convergence speed, and robustness , indicating its potential as a reliable, optimisation technique for a real-world applications shown in Table 2.

V. CONCLUSION

An EV's power flow can be adjusted in several directions with the help of the optimized, isolated DC-DC converter in this research. Dual active bridge (DAB), bidirectional dc-dc, dual active bridge, and unidirectional dc-dc converters are all included in this converter. The power management between the battery and the EV is another function for which the OC was designed. The DAB has chosen the converter's ideal gain parameter. In the suggested method, an EV battery is interfaced with a bidirectional DC-DC converter to enable bidirectional power flow capability. Performance metrics are taken into consideration when evaluating the suggested method, which has been implemented in MATLAB. Furthermore, a comparison has been made with the traditional methods of PSO and fuzzy. By considering the battery lifecycles, the suggested methodology has been assessed. In comparison to traditional methods, it has attained a long battery life (7800 cycles). The best methodology will be used to examine and assess real-time evaluation in the future.

REFERENCES

[1]. S. S. G. Acharige, M. E. Haque, M. T. Arif, N. Hosseinzadeh, K. N. Hasan and A. M. T. Oo, "Review of Electric Vehicle Charging Technologies, Standards, Architectures, and Converter Configurations," in IEEE Access, vol. 11, pp. 41218-41255, 2023, doi: 10.1109/ACCESS.2023.3267164.

[2]. Karneddi, Harish, and Deepak Ronanki. “Reconfigurable Battery Charger with a Wide Voltage Range for Universal Electric Vehicle Charging Applications.” IEEE Transactions on Power Electronics, vol. 38, no. 9, Sep. 2023, pp. 10606-10610. https://doi.org/10.1109/tpel.2023.3289394.

[3]. Mateen, Suwaiba & Amir, Mohammad & Haque, Ahteshamul & Bakhsh, Farhad. (2023). Ultra-fast charging of electric vehicles: A review of power electronics converter, grid stability and optimal battery consideration in multienergy systems. Sustainable Energy, Grids and Networks. 35. 101112. 10.1016/j.segan.2023.101112.

[4]. Saha, Jaydeep & Kumar, Nishant & Panda, Sanjib. (2023). Adaptive GridSupportive Control for Solar-Power Integrated Electric-Vehicle Fast Charging Station. IEEE Transactions on Energy Conversion. PP. 1-11. 10.1109/TEC.2023.3260191.

[5]. Ramesh Jatoth and B. Mangu (2023), Grid-Tied Solar Power Sharing with V2G and G2V Power Exchange with Dual Bridge Integrated Electrical Vehicle. IJEER 11(1), 192-201. DOI: 10.37391/IJEER.110127.

[6]. Varun krishna paravasthu, Balasubbareddy Mallala and B. Mangu (2024), An Enhanced Multi-Objective Evolutionary Optimization Algorithm based on Decomposition for Optimal Placement of Distributed Generation and EV Fast Charging Stations in Distribution System. IJEER 12(2), 575-580. DOI: 10.37391/IJEER-120232.

[7]. Karmaker, Ashish & Hossain, Md. Alamgir & Pota, Hemanshu & Onen, Ahmet & Jung, Jaesung. (2023). Energy Management System for Hybrid Renewable Energy-Based Electric Vehicle Charging Station. IEEE Access. PP. 1-1. 10.1109/ACCESS.2023.3259232.

[8]. Assadi, Seyed & Gong, Zhe & Coelho, Nathan & Zaman, Mohammad & Trescases, Olivier. (2023). Modular Multi-Port Electric-Vehicle DC FastCharge Station Assisted by a Dynamically Reconfigurable Stationary Battery. IEEE Transactions on Power Electronics. PP. 1-12. 10.1109/TPEL.2023.3237622.

[9]. Zanatta, Nicola et al. “A Two-Stage DC-DC Isolated Converter for BatteryCharging Applications.” IEEE Open Journal of Power Electronics 4 (2023): 343-356.

[10]. Woo, Jemin & Han, Seohee & Ahn, Changsun. (2024). SDP-Based Battery Charging Controller for Hybrid Electric Vehicles in Preparation for ZeroEmission Zone Drives. International Journal of Precision Engineering and Manufacturing-Green Technology. 10.1007/s40684-024-00609-9.

Author Profile:

G. YADAIAH has Assistant Professor in ELECTRICAL AND ELECTRONICS ENGINEERING at ANNAMACHARYA INSTITUTE OF TECHNOLOGY & SCIENCES, Hyderabad, India .Has 10 years of teaching experience in engineering colleges He has M.Tech in power Electronics from NOVA college of Engineering & Technology in 2014 and B.Tech in Electrical and Electronics Engineering from ARJUN Institute of Engineering & Technology in 2012.

Areas of interests are WOT (WEB of things), Artificial Intelligence, Cloud computing, Power Electronics, Control Systems, power systems and Electrical machine Electrical circuits.

EMAIL ID: yadaiahacts08@gmail.com

Dr. U. Narender has Associate Professor in ELECTRICAL AND ELECTRONICS ENGINEERING at ANNAMACHARYA INSTITUTE OF TECHNOLOGY& SCIENCES, Hyderabad, India .Has 15 years of teaching experience in engineering colleges He has received his Ph.D. in Electrical Engineering From JJTU University in 2021 and M.Tech in power Electronics from CMR college of Engineering & Technology in 2010 and B.Tech in Electrical and Electronics Engineering from Sindhura Institute of Engineering & Technology in 2006.

Areas of interests are WOT (WEB of things), Artificial Intelligence, Cloud computing, Power Electronics, Control Systems, power systems and Electrical machines.

EMAIL ID: narendercmr1984@gmail.com
narender0866@yahoo.co.in

SCHOLARDETAILS:

INTERNATIONAL JOURNAL OF APPLIED SCIENCE ENGINEERING AND MANAGEMENT

ISSN 2454-9940

www.ijasem.org

Vol 19, Issue 3, 2025

K. RAMESH He Completed B-Tech in VIGNAN INSTITUTE OF TECHNOLOGY AND SCIENCE .His Interested Subjects Are Power Electronics, Electrical Traction, Electrical Drives, Control Systems.
EMAILID: katravathramesh39@gmail.com.